

Interface dynamics from experimental data

Achille Giacometti¹ and Maurice Rossi²

¹*INFM Unitá di Venezia, Dipartimento di Scienze Ambientali, Università di Venezia,
Calle Larga Santa Marta DD 2137, I-30123 Venezia, Italy*

²*Laboratoire de Modélisation en Mécanique, Université de Paris VI, 4 Place Jussieu, F-75252 Paris Cedex 05, France*

(Received 10 February 2000; revised manuscript received 26 April 2000)

An algorithm is envisaged to extract the coupling parameters of the Kardar-Parisi-Zhang (KPZ) equation from experimental data. The method hinges on the Fokker-Planck equation combined with a classical least-square error procedure. It takes properly into account the fluctuations of surface height through a deterministic equation for space correlations. We apply it to the (1+1)-dimensional KPZ equation and carefully compare its results with those obtained by previous investigations. Unlike previous approaches, our method does not require large sizes and is stable under a modification of sampling time of observations. Shortcomings associated with standard discretizations of the continuous KPZ equation are also pointed out and finally possible future perspectives are analyzed.

PACS number(s): 64.60.Ht, 05.40.-a, 05.70.Ln

I. INTRODUCTION

Inverse techniques have a wide range of applicability ranging from geophysics to nonlinear time analysis and statistics [1]. The common philosophy behind these methods is the extraction of equations of motion starting from successive experimental time series of some dynamical variable in addition to basic assumptions such as determinism. If a reasonably general form of the equations is guessed either by symmetry arguments or by general considerations, the “true” parameters are then determined by minimizing a cost function quantifying the distance between experimental observations and corresponding reconstructed quantities, the latter being implicitly dependent upon the parameters. Among such approaches, the least-squares method is the most popular one.

A typical system that can be treated using reconstruction techniques is the case where an *observational noise* is superimposed onto a standard *deterministic* evolution. In this case the system is expected to evolve under the action of the deterministic system and stochasticity comes only from our measurement apparatus. The particular case where the dynamics underlying the system is chaotic has also received considerable attention due to its widespread occurrence in natural systems [2], and the importance of treating the presence of the noise with due care has already been emphasized [3].

The alternative possibility of *dynamical noise* occurs whenever the noise is a built-in component of the equations of motion. This is a far more difficult problem since one has to deal with stochastic rather than deterministic equations. An important such case, which is widespread in nature, is the Langevin dynamics where variables evolve subject both to dissipative generalized forces and to a fluctuating part [4]. In this last instance, the presence of dynamical noise can drastically modify the dynamics and hence hampers the efficiency of the usual reconstruction techniques based on deterministic ideas [5].

In our work, we focus on a particular class of Langevin dynamics that has its origin in a seminal paper on interface

dynamics [6] but has ever since displayed relations with a variety of physical systems, such as, for instance, bacterial colonial growth, immiscible fluids, directed polymers, and superconductors [7].

The Kardar-Parisi-Zhang (KPZ) equation [6] was introduced as a coarse-grained mesoscopic description for the growth of a rough surface under the deposition of particles driven by gravity. The crucial ingredient introduced in the KPZ equation and not present in the corresponding linear counterpart, namely, the Edward-Wilkinson (EW) equation [8], is a nonlinear term which takes into account the fact that the growth is normal to the surface. The KPZ equation can be mapped into various other models. A Cole-Hopf change of variables maps it into a directed polymer diffusion equation subject to a random potential [9], while the identification of the local gradient with a velocity leads to the Burgers equation for a vorticity-free velocity field [10]. Furthermore, it is believed that the KPZ equation has the same large-scale behavior as the Kuramoto-Sivashinsky equation in 1+1 dimensions [11], while in higher dimensionality the situation is much less clear [12]. Nonetheless, in spite of the gigantic effort devoted to the KPZ equation in the past decade, a complete understanding of its properties is still lacking.

The aim of the present paper is to introduce an inverse approach to the KPZ equation. A previous attempt due to Lam and Sander [13] was based on the standard least-squares (LS) reconstruction method. These authors used this approach directly on numerically simulated experimental surfaces without a preventive test of the performance of the method itself. Lam and Shin [14] subsequently showed that the standard discretization used in [13] was not adequate. We shall argue below that, even with the improvements given in [14], the classical identification procedure devised in Ref. [13] is not properly suited for Langevin dynamics since it is based on deterministic equation ideas. By an explicit computation using the LS technique applied to a (1+1)-dimensional KPZ equation, we shall review their method and point out what we consider its main deficiencies.

We then go on to introduce a different approach based on the Fokker-Planck equation (FPE) associated with each

Langevin equation [15,4]. The advantage of this viewpoint is that one can construct *deterministic* relations among correlation functions which, however, still carry information regarding the fluctuating nature of the original quantities. Those equations can then be easily analyzed within a least-squares framework as in the LS method.

The paper is organized as follows. In Sec. II, the KPZ equation is briefly recalled along with its numerical real space approximations in 1+1 dimensions, while the LS approach is reviewed in Sec. III. Section IV contains the basic equations of our modified method, which is then applied in Sec. V. Numerical results are then given in Sec. VI and some concluding remarks are provided in Sec. VII. More technical points are finally confined in the Appendixes. Appendix A shows why the least-square method fails for sufficiently large noise amplitudes and Appendix B presents some results concerning renormalized interfaces and their corresponding renormalized equations.

II. INTERFACE DYNAMICS

We consider a one-dimensional line of total length L and a surface of height $h(x,t)$ at position x and time t . The continuum (1+1)-dimensional KPZ equation then reads

$$\partial_t h(x,t) = c + \nu \partial_x^2 h(x,t) + \frac{\lambda}{2} [\partial_x h(x,t)]^2 + \eta(x,t), \quad (1)$$

where $\eta(x,t)$ is an uncorrelated white noise,

$$\langle \eta(x,t) \eta(x',t') \rangle = 2D \delta(x-x') \delta(t-t'). \quad (2)$$

The average $\langle \rangle$ is taken on different realizations of the noise. In Eqs. (1) and (2), c , ν , λ , and D are coupling parameters [c is often set to zero because of the invariance of Eq. (1) under the rescaling $h \rightarrow h + ct$]. For $\lambda=0$, Eq. (1) reduces to the Edward-Wilkinson equation [8], which can be solved exactly.

In writing Eq. (1) either a regularization in the correlation given in Eq. (2) (such as, for instance, a spatially correlated noise) or the introduction of a minimal length scale a is always tacitly assumed. In the latter case, one is then naturally led to consider a discretization of the continuum equation at a given cutoff length scale a . In that case, (a) the noise term $\eta(x,t)$ is discretized,

$$\eta_i(t) = \sqrt{\frac{D}{a}} \theta_i(t), \quad (3)$$

where $\theta_i(t)$ is a random noise

$$\langle \theta_i(t) \theta_j(t') \rangle = 2 \delta_{i,j} \delta(t-t'), \quad (4)$$

with $\delta_{i,j}$ the Kronecker symbol; and (b) Eq. (1) is written for a discrete variable $h_i(t)$ ($i=1, \dots, N=L/a$) with periodic boundary conditions

$$\frac{dh_i}{dt} = c + \nu_{\text{eff}} F_i^\nu[h] + \frac{\lambda_{\text{eff}}}{2} F_i^\lambda[h] + \sqrt{D_{\text{eff}}} \theta_i(t). \quad (5)$$

Here $\nu_{\text{eff}} = \nu/a^2$, $\lambda_{\text{eff}} = \lambda/a^2$, and $D_{\text{eff}} = D/a$. $F_i^\nu[h]$ and $F_i^\lambda[h]$ are proper discretizations of the linear $\partial_x^2 h$ and non-

linear $(\partial_x h)^2$ terms, respectively. We note that the exact meaning of ‘‘proper discretization’’ has been the object of some investigation [16–19].

In all practical applications, a further temporal discretization [15,20] is also performed on Eq. (5):

$$h_i(t + \delta t) = h_i(t) + \delta t \left(c + \nu_{\text{eff}} F_i^\nu[h(t)] + \frac{\lambda_{\text{eff}}}{2} F_i^\lambda[h(t)] \right) + \sqrt{2D_{\text{eff}} \delta t} r_i, \quad (6)$$

where r_i is a Gaussian random generator of unit variance and δt the discretization time step.

In $d=1+1$ it is known that the steady state solution $P[h]$ for the probability distribution of the heights in the KPZ equation is identical to the EW stationary distribution due to the fluctuation-dissipation theorem [10]. It has been shown [19,21] that the correct stationary discrete probability, namely,

$$P[h] = \mathcal{N}^{-1} \exp \left(-\frac{1}{2} \frac{\nu}{Da} \sum_{i=1}^N (h_i - h_{i+1})^2 \right), \quad (7)$$

where \mathcal{N}^{-1} is a normalization factor, can be obtained by taking

$$F_i^\nu[h] = h_{i+1} + h_{i-1} - 2h_i \quad (8)$$

and

$$F_i^\lambda[h] = \frac{1}{3} [(h_{i+1} - h_i)^2 + (h_{i+1} - h_i)(h_i - h_{i-1}) + (h_i - h_{i-1})^2]. \quad (9)$$

The standard choice $F_i^\lambda[h] = (1/4)(h_{i+1} - h_{i-1})^2$, on the other hand, fails to reproduce Eq. (7) and suffers other problems as well [18]. A necessary (albeit not sufficient) condition for identification with the continuum counterpart Eq. (1) is clearly that the correct steady state (i.e., independent of λ) is recovered. For this reason, we shall exploit for our identification procedure as well as for the LS scheme Eqs. (8) and (9) hereafter, instead of the standard choice that was used in [13].

III. LEAST-SQUARES ERROR MODEL METHOD

Before introducing our method we first review the LS error method used in Ref. [13]. We consider experimental surfaces coarse grained at length scale a described by the interface heights $h_i^{\text{obs}}(t)$ ($i=1, \dots, N$), which are sampled M times, i.e., at discrete times $t = t_k = k\Delta t$ ($k=1, \dots, M+1$). Note that the sampling time Δt is the time interval between two experimental observations and it is clearly different from the discretization time δt of Eq. (6). For surfaces obtained by numerical simulations Δt is typically a multiple of δt . We note that, in Ref. [13], the authors used Δt equal to δt which is a rather particular case.

For the sake of simplicity, we assume here that measurements are free from observational noise. It must be emphasized that, in the presence of measurement noise, our method performs *a priori* better than the LS scheme since it is based

on spatial-averaged values, which are less affected by errors on local height measurements.

Our purpose is to determine the coefficients c , ν , λ , and D at the given length scale a in Eq. (3). Let us first neglect the dynamical noise in Eq. (5). We then obtain a standard identification problem of the coupling parameters governing a deterministic nonlinear equation which can be cast in the compact form

$$\frac{dh_i}{dt} = \sum_{\alpha=1}^p \mu_\alpha F_i^\alpha[h], \quad (10)$$

where in the present case $p=3$ and $\mu_1=c$, $\mu_2=\nu_{\text{eff}}$, $\mu_3=\lambda_{\text{eff}}$, and Eqs. (8) and (9) are used for $F_i^2[h]$ and $F_i^3[h]$ whereas $F_i^1[h]=1$.

Optimal parameters are then determined by minimizing a cost function \mathcal{J} such as the sum-square difference

$$\mathcal{J} = \frac{1}{NM} \sum_{k=1}^M \sum_{i=1}^N [h_i^{\text{obs}}(t_{k+1}) - h_i^{\text{pred}}(t_{k+1})]^2, \quad (11)$$

which quantifies the distance between experimental observations $h_i^{\text{obs}}(t_k)$ and equivalent reconstructed quantities $h_i^{\text{pred}}(t_k)$. The latter quantities are computed from Eq. (10) for given parameters and are thus generally implicit functions of the parameters. However, if the sampling time Δt is small enough, then $F_i^\alpha[h]$ are nearly constant between two measurements and the amplitudes $h_i^{\text{pred}}(t_{k+1})$ can be related to the parameters μ_α by

$$h_i^{\text{pred}}(t_{k+1}) = h_i^{\text{obs}}(t_k) + \Delta t \sum_{\alpha=1}^p \mu_\alpha F_i^\alpha[h^{\text{obs}}(t_k)]. \quad (12)$$

In this case, the cost function $\mathcal{J}(\{\mu\})$ itself becomes explicit and quadratic in the parameters. Optimal parameters can thus be evaluated through a simple matrix inversion. Indeed, the extremal value of \mathcal{J} is inferred from

$$\left. \frac{\partial \mathcal{J}}{\partial \mu_\alpha} \right|_{\mu^*} = 0. \quad (13)$$

The solution for the optimal parameters $\{\mu^*\}$ is then given by a matrix equation,

$$\mu_\alpha^* = \sum_{\beta=1}^p A_{\alpha\beta}^{-1} B_\beta, \quad (14)$$

where we have defined

$$A_{\alpha\beta} = \frac{1}{NM} \sum_{k=1}^M \sum_{i=1}^N F_i^\alpha F_i^\beta, \quad (15)$$

$$B_\alpha = \frac{1}{NM} \sum_{k=1}^M \sum_{i=1}^N \left(\frac{h_i^{\text{obs}}(t_{k+1}) - h_i^{\text{obs}}(t_k)}{\Delta t} \right) F_i^\alpha, \quad (16)$$

and where functions F_i^α are clearly expressed at $h_1^{\text{obs}}(t_k), \dots, h_N^{\text{obs}}(t_k)$.

This classical least-squares method is an easy and natural approach and it works fairly well in the absence of any noise.

In the presence of noise, however, it has its main drawback in the fact that it approximates time derivatives by finite differences. If the dynamics is governed by a deterministic equation and measurements are performed with a negligible observational noise, this simply imposes the choice of a sampling time much smaller than the characteristic or relaxation time of the process.

Lam and Sander [13] assumed that if the sampling time Δt is small enough, the above method could be extended to a Langevin equation (i.e., with dynamical noise). The amplitude of the noise can then be inferred from Eq. (11) when J is taken at the minimum values of the parameters, that is,

$$D = \frac{1}{2\Delta t} aJ(\{\mu^*\}). \quad (17)$$

However, it has already been observed in dynamical systems that even with pure measurement noise the above method can cause large errors. This is expected to be the case for dynamical noise as well. Two main reasons for this can be advocated. First, if Δt is too large, the linear approximation (12) which explicitly relates the observed quantities breaks down. Because of the dynamical noise term, this happens *a priori* for shorter time intervals in a Langevin equation compared with its deterministic counterpart. Second, even in the favorable case in which Δt is small, such a method is efficient only if large sizes and small noise amplitudes are used. This is explained in Appendix A, where a simple zero-dimensional case is explicitly worked out with the method of Lam and Sander.

IV. STOCHASTIC APPROACH FOR MODEL IDENTIFICATION

We now turn to our method, which is based on the simple observation that all the information present in the Langevin equation (5) is also contained in the corresponding Fokker-Planck equation [15]:

$$\partial_t P[h, t] = \sum_{i=1}^N D_{\text{eff}} \frac{\partial^2}{\partial h_i^2} P[h, t] - \sum_{i=1}^N \frac{\partial}{\partial h_i} (F_i[h] P[h, t]), \quad (18)$$

where

$$F_i[h] = c + \nu_{\text{eff}} F_i^\nu[h] + \frac{1}{2} \lambda_{\text{eff}} F_i^\lambda[h] \quad (19)$$

and [22]

$$P[h, t] = \left\langle \prod_{i=1}^N \delta(h_i - h_i(t)) \right\rangle, \quad (20)$$

where the solution $h_i(t)$ is associated to a particular noise configuration $\theta_i(t)$.

In Eq. (18) the second term on the right-hand side characterizes the deterministic behavior of the system whereas the first term contains stochastic effects. We derive a first general equation involving the parameters c and λ . Using Eq. (18), the time derivative of the ensemble average of $h_i(t)$ can easily be shown to be

$$\frac{d\langle h_i(t) \rangle}{dt} = \int \mathcal{D}h F_i[h] P[h, t], \quad (21)$$

where $\mathcal{D}h \equiv \prod_{i=1}^N dh_i$. If we denote by $g^{(1)}(t) = (1/N) \sum_i \langle h_i(t) \rangle$ the mean height at time t averaged over the noise, its time derivative can be written after some simple algebra as

$$\frac{dg^{(1)}(t)}{dt} = c + \frac{\lambda_{\text{eff}}}{6} [2g_0^{(2)}(t) + g_1^{(2)}(t)], \quad (22)$$

where we have defined

$$g_i^{(2)}(t) = \frac{1}{N} \sum_{i=1}^N \langle \delta h_i(t) \delta h_{i+t}(t) \rangle \quad (23)$$

in the variables $\delta h_i = h_i - h_{i+1}$. Note that there are only $N - 1$ independent δh_i variables due to periodic boundary conditions and to the fact that $\sum_{i=1}^N \delta h_i = 0$.

The above result prompts a convenient change of variables from h_1, \dots, h_N to $\delta h_1, \dots, \delta h_{N-1}, \bar{h} \equiv 1/N \sum_{i=1}^N h_i$, followed by an integration over \bar{h} . Physically, this is related to the fact that our system is infinitely degenerate with respect to the average height. Note that the stationary probability Eq. (7) is now Gaussian and well defined in the new variables $\delta h_1, \dots, \delta h_{N-1}$. The corresponding probability $\tilde{P}[\delta h]$ is the solution of a modified FPE:

$$\begin{aligned} \partial_t \tilde{P}[\delta h, t] = & 2D_{\text{eff}} \sum_{i=1}^{N-1} \frac{\partial^2}{\partial \delta h_i^2} \tilde{P}[\delta h, t] \\ & - \sum_{i=1}^{N-1} \frac{\partial}{\partial \delta h_i} (G_i[\delta h] \tilde{P}[\delta h, t]) \\ & - 2D_{\text{eff}} \sum_{i=2}^{N-1} \frac{\partial^2}{\partial \delta h_i \partial \delta h_{i-1}} \tilde{P}[\delta h, t], \end{aligned} \quad (24)$$

where we have defined

$$G_i^\lambda = F_i - F_{i+1} = \nu_{\text{eff}} G_i^\nu + \frac{1}{2} \lambda_{\text{eff}} G_i^\lambda, \quad (25)$$

with

$$G_i^\nu = \delta h_{i+1} + \delta h_{i-1} - 2\delta h_i \quad (26)$$

and

$$G_i^\lambda = \frac{1}{3} [\delta h_{i-1}^2 - \delta h_{i+1}^2 - \delta h_i (\delta h_{i+1} - \delta h_{i-1})]. \quad (27)$$

We are now in a position to derive our second basic result.

Integrating Eq. (25) over all variables but (say) δh_j , one gets, for the single variable probability

$$p(\delta h_j) = \int \mathcal{D}\delta h_j \tilde{P}[\delta h, t], \quad (28)$$

where the shorthand notation $\mathcal{D}\delta h_j = \prod_{i \neq j=1}^{N-1} d\delta h_i$ was again exploited, the following equation:

$$\partial_t p(\delta h_j, t) = 2D_{\text{eff}} \frac{\partial^2}{\partial \delta h_j^2} p(\delta h_j, t) - \frac{\partial}{\partial \delta h_j} \pi(\delta h_j, t), \quad (29)$$

where the nonlocal term $\pi(\delta h_j, t)$ is defined as

$$\pi(\delta h_j, t) = \int \mathcal{D}\delta h_j G_j[\delta h] \tilde{P}[\delta h, t]. \quad (30)$$

The last step is to introduce the Fourier transform of $p(\delta h_j, t)$, which can be reckoned as a generating function for all moments of the distribution. Specifically, on defining

$$\hat{p}_j(q, t) = \int_{-\infty}^{+\infty} d\delta h_j e^{iq\delta h_j} p(\delta h_j, t), \quad (31)$$

we find a simple equation for the average $\hat{p}(q, t)$ over all sites of $\hat{p}_j(q, t)$:

$$\partial_t \hat{p}(q, t) = -2D_{\text{eff}} q^2 \hat{p}(q, t) - iq \hat{\pi}(q, t), \quad (32)$$

in which $\hat{\pi}(q, t)$ is the Fourier transform of $\pi(\delta h_j, t)$ averaged over all sites. One can then expand Eq. (32) in powers of q and obtain an infinite hierarchy (closure problem) in the correlation functions. The first two nontrivial orders [$O(q^2)$ and $O(q^3)$] are

$$\frac{dg_0^{(2)}(t)}{dt} = 4\nu_{\text{eff}} [g_1^{(2)}(t) - g_0^{(2)}(t)] + 4D_{\text{eff}} \quad (33)$$

and

$$\begin{aligned} \frac{dg_{00}^{(3)}(t)}{dt} = & -3\nu_{\text{eff}} [g_{11}^{(3)}(t) + g_{01}^{(3)}(t) - 2g_{00}^{(3)}(t)] \\ & + \frac{1}{2} \lambda_{\text{eff}} [g_{001}^{(4)}(t) - g_{111}^{(4)}(t)], \end{aligned} \quad (34)$$

where we have defined the following higher order correlation functions:

$$g_{lm}^{(3)}(t) = \frac{1}{N} \sum_{i=1}^N \langle \delta h_i(t) \delta h_{i+l}(t) \delta h_{i+m}(t) \rangle, \quad (35)$$

$$g_{lmn}^{(4)}(t) = \frac{1}{N} \sum_{i=1}^N \langle \delta h_i(t) \delta h_{i+l}(t) \delta h_{i+m}(t) \delta h_{i+n}(t) \rangle. \quad (36)$$

It is worth mentioning that λ does not explicitly appear in Eq. (33). As one can explicitly check, this is a feature associated with the particular discretization Eq. (9) and it would *not* have been the case had we used the standard discretization for $F_i^\lambda[h]$. This is clearly related, in turn, to the fact that the steady state probability distribution Eq. (7) is independent of λ . We also note that in the (1+1)-dimensional case we are considering, the explicit steady state solution of Eq. (32) is known, and depends only on a single parameter D/ν . As a consequence, the steady state version of Eq. (32) cannot be used here to identify ν and D . In the (2+1)-dimensional case, where such a peculiar feature is not present, the station-

ary solution depends on λ as well and parameter identification can exploit the steady state analog equation.

V. PARAMETER IDENTIFICATION

Our aim is to implement an identification procedure which could be exploited in real experiments. For this reason, we assume that the experimental surface is constituted by a finite number of sites N with lattice spacing a (corresponding to a size $L=Na$), and it is measured during a finite time T_{obs} every sampling time Δt . Again, Δt is *a priori* different from the discretization time δt when the data are produced numerically (note that in real experiments δt is not even defined). We shall test the robustness and efficiency of the scheme with respect to the size L and sampling time Δt .

Identification methods are often based on minimizing a cost function defined through dynamical constraints. This is clearly the case of the least-squares method as explained in Sec. III. Here we derive dynamical constraints using Eqs. (22) and (33), which contain information from the original Langevin equation, including mean values and fluctuations around mean values. The present identification is thus based on *deterministic* equations. This constitutes a crucial difference with respect to the previous reconstruction method [13] directly based on *stochastic* equations. Another important feature is that the observed quantities we use in our reconstruction scheme are dealing with averaged site values. Hence the fluctuations of all these terms, which derive from stochastic quantities, are *reduced* typically by a factor $1/\sqrt{N}$, and self-averaging is expected to be more effective.

Let us derive the constraints we use. First, the total observation time T_{obs} is divided into q equal slices $[T_1, T_2], \dots, [T_q, T_{q+1}]$ with $\Delta T = T_{j+1} - T_j$. Let us integrate Eqs. (22) and (33) on each slice $[T_j, T_{j+1}]$:

$$\frac{\Delta g^{(1)}}{T_{j+1} - T_j} = c + \frac{\lambda_{\text{eff}}}{6} \frac{1}{T_{j+1} - T_j} \int_{T_j}^{T_{j+1}} dt [2g_0^{(2)}(t) + g_1^{(2)}(t)], \quad (37)$$

$$\begin{aligned} \frac{\Delta g_0^{(2)}}{T_{j+1} - T_j} &= 4\nu_{\text{eff}} \frac{1}{T_{j+1} - T_j} \int_{T_j}^{T_{j+1}} dt [g_1^{(2)}(t) - g_0^{(2)}(t)] \\ &+ 4D_{\text{eff}}. \end{aligned} \quad (38)$$

If the functions and integrals in Eqs. (37) and (38) are computed using experimental data, these discrete equations provide $2q$ relations between the parameters to identify. From these constraints, two cost functions are built in a way already described in Sec. III with $p=2$. The corresponding 2×2 equations then yield c and λ from one cost function and ν and D from the other.

We now explain how the functions and integrals in Eqs. (37) and (38) are obtained experimentally. Starting with the *same* initial surface, e.g., a flat surface, we will grow the surface \mathcal{R} times. Because of the stochastic nature of the phenomenon, this produces \mathcal{R} different observations or realizations of the same process. Such a procedure, which can be performed very easily in real experiments, allows the computation, at sampling times $t=t_k=k\Delta t$ ($k=1, \dots, M+1$), of $[g^{(1)}]_{\text{expt}}$, $[g_0^{(2)}]_{\text{expt}}$, and $[g_1^{(2)}]_{\text{expt}}$. Indeed, these quantities are the averages over \mathcal{R} different realizations of the spa-

tial average height and correlations of the first neighbors. The number \mathcal{R} of realizations need not be large: if the total number N of sites is sufficiently large, the experimental values are rather close to the corresponding theoretical predictions $g^{(1)}(t)$, $g_0^{(2)}(t)$, and $g_1^{(2)}(t)$. From these functions sampled every $t=t_k=k\Delta t$, the integrals in Eqs. (37) and (38) can be efficiently evaluated for small sampling time Δt . In this case, the smooth functions $[g^{(1)}]_{\text{expt}}$, $[g_0^{(2)}]_{\text{expt}}$, and $[g_1^{(2)}]_{\text{expt}}$ can be approximated on the whole time interval $[T_1, T_{q+1}]$ by a standard curve fitting algorithm which gives as a by-product the time integrals. This method does impose a constraint on the sampling time Δt . However, this constraint is substantially weaker with respect to that imposed by the LS method, as we will show below. This is a considerable advantage of our procedure.

Two remarks are in order here. First one expects the result to be independent of the number of slices q provided that q satisfies the following two constraints. On the one hand q should be greater than 2 (since two parameters are identified per cost function) and on the other hand it should be less than $M=T_{\text{obs}}/\Delta t$ so that ΔT cannot be less than the sampling time Δt . Second, the identification of ν and D could be achieved by using Eq. (32) rather than Eq. (33). We shall see that in our approach the two equations yield virtually identical results.

VI. RESULTS

In order to test the potentiality of the different identification methods, we produce experimental data by simulating Eq. (5) with a standard Euler time integration algorithm with time step $\delta t=0.01$, lattice spacing $a=1$, and parameters $\nu=D=1$ and $\lambda=3$. These are the same values used in Ref. [14]. The time step is expected to be sufficiently small to cause no instability problems and the nonlinear term λ is big enough to be well inside the KPZ phase. We find it interesting to repeat each calculation a few times (typically five) to give an estimate of the error bars to be associated with each parameter value (this was missing in previous work).

A. LS method

Let us compute the parameters using the original LS method with the spatial and temporal discretization of Eqs. (5) and (6). We exploit the same trick used in Ref. [14] in which a KPZ surface of size $2L$ is obtained by a magnification of a fully relaxed surface of size L where the height is rescaled by a factor 2^α ($\alpha=0.5$) and linearly interpolated. The surface obtained is then relaxed to stationarity before the next magnification is attempted. However, unlike Ref. [14] where a single surface of size $L=32\,768$ was computed, we consider $L=512, 1024, 2048$, and 4096 and linearly extrapolate the results to the limit $L \rightarrow \infty$. The calculation is repeated for increasing values of $s=\Delta t/\delta t$ in order to display the crucial weakness of the method as explained before. Figure 1 depicts the results for the parameter ν at finite L . Similar trends are present for λ and D . The extrapolated values at $L \rightarrow \infty$ are reported in Table I. The gradual decrease in the precision of the reconstructed parameters is apparent and it shows the loss of accuracy of the LS method as Δt increases, as previously noted.

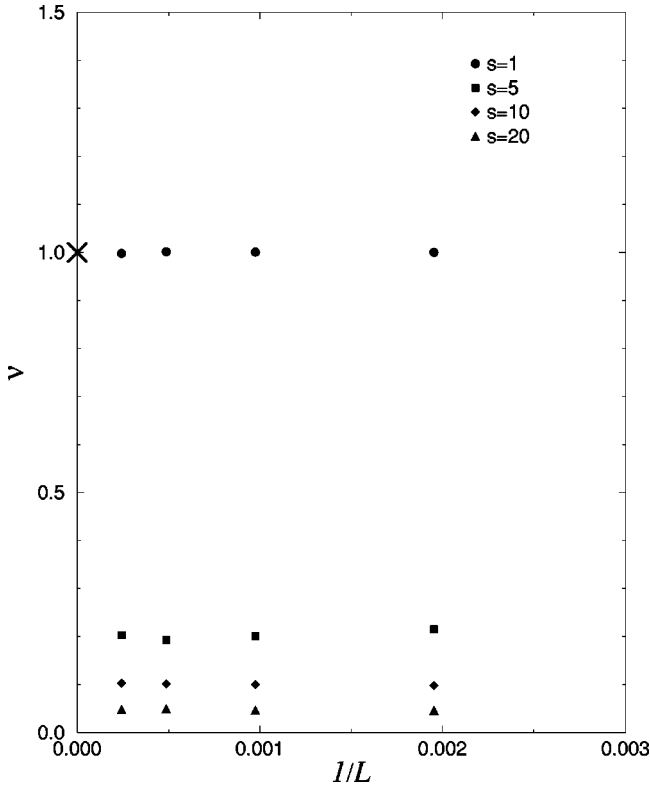


FIG. 1. The coupling parameter ν for increasing lattice sizes $L = 512, 1024, 2048, 4096$, in the original steady state LS method. All quantities are in dimensionless form. Error bars are of the order of the symbol sizes and are consequently not displayed. Different curves refer to increasing values of the ratio $s = \Delta t / \delta t$. The cross (\times) indicates the exact value of the parameter $\nu = 1$.

We also considered the LS method when the reconstructed quantities are computed at time intervals ΔT that are multiples of the sampling time Δt . In fact, this test was also carried out by the authors of Ref. [14] (in their notation $\tau = \Delta T$ and $\Delta t = \delta t$) and it will constitute a further source of comparison with our alternative stochastic method (see below). Even in this case there is a decrease in the performance of the procedure as the ratio $r = \Delta T / \Delta t$ increases, consistent with the results of Ref. [14]. The corresponding extrapolated values are reported in Table II.

B. Stochastic approach

For a more convenient comparison with the LS method, we use the same sizes and statistics (five different configurations for each size). Our calculations are carried out in the *transient* rather than in the *steady* state and are therefore

TABLE I. Extrapolated values of coupling parameters $\nu(\infty)$, $\lambda(\infty)$, and $D(\infty)$ as a function of $s = \Delta t / \delta t$ (see text) as computed from the original LS method (at steady state).

$\Delta t / \delta t$	$\nu(\infty)$	$\lambda(\infty)$	$D(\infty)$
1	0.999 ± 0.003	2.980 ± 0.005	1.000 ± 0.001
5	0.194 ± 0.004	0.595 ± 0.015	0.200 ± 0.001
10	0.103 ± 0.004	0.319 ± 0.008	0.100 ± 0.001
20	0.049 ± 0.002	0.139 ± 0.004	0.050 ± 0.001

TABLE II. Extrapolated values of coupling parameters $\nu(\infty)$, $\lambda(\infty)$, and $D(\infty)$ as a function of $r = \Delta T / \Delta t$ (see text) as computed from the original LS method (at steady state).

$\Delta T / \Delta t$	$\nu(\infty)$	$\lambda(\infty)$	$D(\infty)$
1	0.999 ± 0.003	2.980 ± 0.005	1.000 ± 0.001
5	0.996 ± 0.002	2.817 ± 0.004	0.928 ± 0.001
10	0.917 ± 0.002	2.627 ± 0.006	0.853 ± 0.001
20	0.855 ± 0.002	2.308 ± 0.006	0.757 ± 0.001
50	0.650 ± 0.001	1.558 ± 0.006	0.653 ± 0.002

much less time consuming. Again the results are obtained for $L = 512, 1024, 2048$, and 4096 and linearly extrapolated to $L \rightarrow \infty$. For a comparison with the previous calculation, the outcomes for the parameter ν at different sizes L are plotted in Fig. 2 for increasing values of the ratio $s = \Delta t / \delta t$, and the corresponding extrapolated values are reported in Table III. One can see that the parameter values are rather insensitive to the changing the ratio $s = \Delta t / \delta t$, as expected. Next we checked the performance of our method with respect to increase of the ratio $r = \Delta T / \Delta t$. This is reported in Table IV. As expected, our method outperforms the LS one in all situations.

Since the LS method could in principle be carried out in transient rather than in steady state conditions, one might wonder how it would perform in this case. To this end we recomputed the parameters using the LS method under these

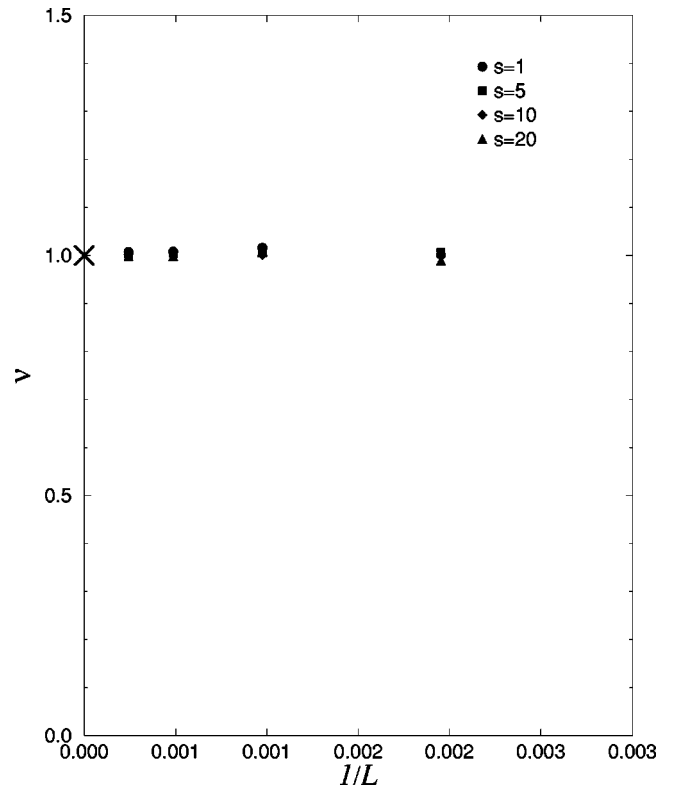


FIG. 2. The coupling parameter ν for increasing lattice sizes $L = 512, 1024, 2048, 4096$, as obtained from our reconstruction method. Error bars are of the order of the symbol sizes and are consequently not displayed. Different curves refer to increasing values of the ratio $s = \Delta t / \delta t$. The cross (\times) indicates the exact value of the parameter $\nu = 1$.

TABLE III. Extrapolated values of coupling parameters $\nu(\infty)$, $\lambda(\infty)$, and $D(\infty)$ as a function of $s = \Delta t / \delta t$ as computed from our stochastic approach in the transient state.

$\Delta t / \delta t$	$\nu(\infty)$	$\lambda(\infty)$	$D(\infty)$
1	1.009 ± 0.002	3.047 ± 0.016	1.026 ± 0.001
5	1.008 ± 0.007	3.015 ± 0.006	1.003 ± 0.007
10	1.035 ± 0.011	2.993 ± 0.010	1.018 ± 0.011
20	0.997 ± 0.020	3.001 ± 0.005	0.978 ± 0.010

conditions and found that the predicted values are far off with respect to the exact ones. For instance, for $L = 4096$ a typical run yields $\nu \sim 0.36$, $\lambda \sim 0.68$, and $D \sim 0.005$, to be compared with a typical result obtained with our method $\nu \sim 0.99$, $\lambda \sim 2.98$, and $D \sim 1.01$.

As a final cross-check of our method, we recomputed the parameters in the same situation as before but using Eq. (32) rather than Eq. (33) to extract ν and D , and found nearly identical values.

C. Coarse graining and KPZ real discretization

The application of this method to experimental surfaces assumes that the system is described by a KPZ-like dynamics. In this case, besides being able to address the issue of whether or not they belong to the KPZ universality class, one would be able to provide a numerical estimates of the coupling parameters, which are usually overlooked in studies focusing only on the universality class.

Following Lam and Sander [13], we produce an interface based on the KPZ discretized model Eq. (5), which is then smoothed by introducing the (discrete) Fourier transform of the heights

$$\hat{h}_{q_n}(t) = a \sum_{i=1}^N e^{-iq_n x_i} h_i(t). \quad (39)$$

A coarse-graining surface at level $a_s = ba$ can then be achieved by simply setting to zero all wavelength components $\hat{h}_{q_n}(t)$ with $q \geq N_s = L/a_s$ and transforming back to real space. The smoothed surface obtained is then assumed to be governed by a KPZ equation (renormalizability property). This new KPZ dynamics can then be reconstructed along lines similar to those described above before a further time step is carried out on the original surface.

With $b = 2$, $\Delta T / \Delta t = 1$, and sizes up to $L = 8192$ averaged over five configurations as before, we find $\nu = 1.09 \pm 0.04$,

TABLE IV. Extrapolated values of coupling parameters $\nu(\infty)$, $\lambda(\infty)$, and $D(\infty)$ as a function of $r = \Delta T / \Delta t$ as computed from our stochastic approach in the transient state.

$\Delta T / \Delta t$	$\nu(\infty)$	$\lambda(\infty)$	$D(\infty)$
1	1.009 ± 0.002	3.047 ± 0.016	1.026 ± 0.001
5	1.003 ± 0.003	3.005 ± 0.010	1.057 ± 0.003
10	1.003 ± 0.001	3.030 ± 0.007	1.023 ± 0.001
20	0.998 ± 0.002	3.014 ± 0.009	1.016 ± 0.001
50	0.991 ± 0.003	3.017 ± 0.006	1.010 ± 0.003

$\lambda = 3.27 \pm 0.05$, and $D = 0.88 \pm 0.03$. Higher values of b result in poorer and poorer agreement with the expected values even with larger lattice sizes. The same feature is also present in the original LS procedure as we explicitly checked. In fact, this is a general deficiency of the real space discretization as explained in Appendix B: the finite size difference has lost some renormalizability property of the original KPZ continuum equation.

VII. CONCLUSIONS

In this paper, we discuss a method for extracting the coupling parameters from a nonlinear Langevin equation starting from experimental surfaces representing successive snapshots of the system. We apply this scheme to the KPZ equation in 1+1 dimensions (although it could be extended to any dimensions) and compare it with the previous approach of Ref. [13], finding the following differences. First of all it does not require large sizes and it is well suited for a transient state. This is expected to be a considerable advantage, notably in numerical work, since the typical time required to reach a steady state increases as L^z where z is the dynamical exponent [$3/2$ in the (1+1)-dimensional KPZ case]. We have explicitly shown how the LS method, which works rather well in the aforementioned conditions, fails to provide sensible answers otherwise. Most important, however, is the fact that our approach is stable under changes of the sampling time, unlike the LS method, which is not. We stress the importance of this feature since in typical experimental situations the sampling time is an externally tuned parameter that has nothing to do with the evolution time of the system. We have discussed the reasons why this is so and provide an intuitive heuristic argument showing why the LS scheme is *not* expected to work under these more realistic conditions. Finally, we implemented a coarse-graining procedure in order to be able to apply our method to experimentally generated profiles. We showed that the agreement with the expected values is much poorer in the present case, and we further argued that *any* real space based approach is doomed to run into this problem, the reason being that these approaches do not have a correct renormalization behavior under coarse graining, as explained in Appendix B. We have recently devised an alternative approach based on a Fourier-based scheme, which avoids discretization problems. The results of this will be the subject of a forthcoming publication.

ACKNOWLEDGMENTS

This work was supported by a joint CNR-CNRS exchange program No. 5274. One of us (A.G.) acknowledges financial support by MURST and INFN.

APPENDIX A: A SIMPLE SOLVABLE EXAMPLE

This Appendix shows, on a simple and solvable example which is a zero-dimensional analog of Eq. (1), that the method of least squares can be hampered by the presence of dynamical noise. Let us assume that the scalar variable $X(t)$ is governed by the following Langevin equation:

$$\frac{dX}{dt} = B(X) + \mu G(X) + \eta(t), \quad (\text{A1})$$

where B and G are prescribed functions, and $\eta(t)$ is an uncorrelated white noise

$$\langle \eta(t) \eta(t') \rangle = 2D \delta(t - t'). \quad (\text{A2})$$

For simplicity, we assume that (a) measurement noise is negligible, (b) the observed time series $X^{\text{obs}}(t_k)$ with $t_k = k\Delta t$ ($k = 1, \dots, M+1$) has been produced by the dynamical system (A1) with the value $\mu = 0$. We ask whether the least-squares method is capable of identifying the correct coupling parameter $\mu = 0$.

On the one hand, the least-squares method first assumes that the data are produced by the deterministic counterpart of Eq. (A1) with an unknown parameter μ . In discrete times, this yields a ‘‘predicted’’ value given by

$$X^{\text{pred}}(t_{k+1}) = X^{\text{obs}}(t_k) + \Delta t [B(X^{\text{obs}}(t_k)) + \mu G(X^{\text{obs}}(t_k))]. \quad (\text{A3})$$

On the other hand, the ‘‘observed’’ value is given, if the sampling time is small enough, by the discrete time counterpart of Eq. (A1) with $\mu = 0$:

$$X^{\text{obs}}(t_{k+1}) = X^{\text{obs}}(t_k) + \Delta t B(X^{\text{obs}}(t_k)) + r(t_k) \sqrt{2D\Delta t}, \quad (\text{A4})$$

where $r(t_k)$ is a Gaussian random generator of unit variance.

Using both experimental observations $X^{\text{obs}}(t_k)$ and reconstructed quantities $X^{\text{pred}}(t_k)$, a cost function can be constructed:

$$\mathcal{J} = \frac{1}{M} \sum_{k=1}^M [X^{\text{obs}}(t_{k+1}) - X^{\text{pred}}(t_{k+1})]^2. \quad (\text{A5})$$

Using Eqs. (A3) and (A4), the cost function is readily rewritten as

$$\mathcal{J} = \frac{1}{M} \sum_{k=1}^M [\Delta t \mu G(X^{\text{obs}}(t_k)) - r(t_k) \sqrt{2D\Delta t}]^2. \quad (\text{A6})$$

The minimum value of \mathcal{J} then satisfies the extremality condition

$$\left. \frac{\partial \mathcal{J}}{\partial \mu} \right|_{\mu^*} = 0, \quad (\text{A7})$$

which provides the value

$$\mu^* = \sqrt{\frac{2D}{\Delta t}} \frac{(1/M) \sum_{k=1}^M r(t_k) G(X^{\text{obs}}(t_k))}{(1/M) \sum_{k=1}^M G^2(X^{\text{obs}}(t_k))}. \quad (\text{A8})$$

Let us estimate the two sums appearing in Eq. (A8). Because of self-averaging, the denominator can clearly be rewritten as

$$\frac{1}{M} \sum_{k=1}^M G^2(X^{\text{obs}}(t_k)) \approx \langle G^2 \rangle, \quad (\text{A9})$$

the average being over the noise η . The second sum can be separated into two contributions,

$$\begin{aligned} & \frac{1}{M} \sum_{k=1}^M [r(t_k) G(X^{\text{obs}}(t_k))] \\ &= \frac{1}{M} \sum_{k=1}^M r(t_k) [G(X^{\text{obs}}(t_k)) - \langle G \rangle] + \frac{\langle G \rangle}{M} \sum_{k=1}^M r(t_k), \end{aligned} \quad (\text{A10})$$

where using the central limit theorem (CLT) [4] we have that

$$\frac{\langle G \rangle}{M} \sum_{k=1}^M r(t_k) \approx \frac{\langle G \rangle}{\sqrt{M}} r_1, \quad (\text{A11})$$

where r_1 is a random variable of unit variance. In Eq. (A10), each term of the first sum of the right-hand side (rhs) is a random variable which is a product of two independent random variables of zero mean and variance, respectively equal to 1 and $\sigma = \langle G^2 \rangle - \langle G \rangle^2$. A similar argument based on the CLT applies to the evaluation of the first term of the rhs since it is again a sum of M random variables with zero average, which implies that

$$\frac{1}{M} \sum_{k=1}^M r(t_k) [G(X^{\text{obs}}(t_k)) - \langle G \rangle] \approx \frac{\sqrt{\sigma}}{\sqrt{M}} r_2, \quad (\text{A12})$$

where r_2 is a random variable of unit variance. Instead of the true value one then finds

$$\mu^* \approx \frac{\sqrt{2D}}{\sqrt{M\Delta t}} \frac{\max(\sqrt{\sigma}, \langle G \rangle)}{\langle G^2 \rangle}. \quad (\text{A13})$$

With nonvanishing amplitudes D , the noise hence causes errors for small Δt unless large statistics are considered.

APPENDIX B: NONRENORMALIZABILITY OF REAL SPACE DISCRETIZATIONS

Let us consider a one-dimensional surface defined on a lattice of length $L = Na$ (a being the lattice spacing and N being the total number of sites), which is identified by h_1, \dots, h_N at positions $x_1 = a, \dots, x_N = Na$ and has periodic boundary conditions. If we assume a KPZ dynamics, then the equation of motion is given by Eq. (5) and its stationary state by Eq. (7). Let us introduce the (discrete) Fourier transform \hat{h}_q so that

$$h_i(t) = \frac{1}{L} \sum_{n=-N/2}^{N/2} e^{iq_n x_i} \hat{h}_{q_n}(t), \quad (\text{B1})$$

and conversely

$$\hat{h}_{q_n}(t) = a \sum_{i=1}^N e^{-iq_n x_i} h_i(t). \quad (\text{B2})$$

By using the relation

$$\sum_{i=1}^N e^{i(q_n - q_m)x_i} = N \delta_{n,-m}, \quad (\text{B3})$$

it is easy to show that the correct corresponding relation of Eq. (7) for the stationary distribution is

$$\widehat{P}_a[\hat{h}] = \mathcal{N}^{-1} \exp\left(-\frac{1}{2} \frac{\nu}{DL} \sum_{n=-N/2}^{N/2} q_n^2 |\hat{h}_{q_n}|^2\right). \quad (\text{B4})$$

In Eq. (B4) the continuum limit $a \rightarrow 0$ is simply achieved by letting $N \rightarrow \infty$.

We now recall that the proper variables to be used in this context are the $\delta h_i = h_i - h_{i+1}$, whose Fourier transform $\delta \hat{h}_{q_n}$ are related to the Fourier transform \hat{h}_{q_n} of the heights by

$$\delta \hat{h}_{q_n} = \hat{h}_{q_n} (1 - e^{iq_n a}). \quad (\text{B5})$$

We can exploit the periodic boundary conditions to extend the $N-1$ sites to N (bearing in mind, however, that only $N-1$ are independent) and use the the fact that

$$\frac{1}{a} \sum_{i=1}^N \delta h_i^2 = \frac{1}{La^2} \sum_{n=-N/2}^{N/2} |\delta \hat{h}_{q_n}|^2, \quad (\text{B6})$$

to rewrite the probability (B4) in the alternative form

$$\widehat{P}_a[\hat{h}] = \mathcal{N}^{-1} \exp\left(-\frac{1}{2} \frac{\nu}{DL a^2} \sum_{n=-N/2}^{N/2} |\hat{h}_{q_n} (1 - e^{iq_n a})|^2\right). \quad (\text{B7})$$

In the continuum limit $a \rightarrow 0$ one can explicitly check that Eq. (B7) is equivalent to Eq. (B4) by expanding the term $e^{iq_n a}$ in powers of a and keeping the lowest nonvanishing order $O(a)$. Nevertheless, Eq. (B7) leads to problems when one tries to coarse-grain the surface. Indeed, suppose we now perform a smoothing of the lattice of a factor b to obtain a new lattice constant $a_s = ba$ and a decreased number of sites $N_s = N/b$. This amounts to setting to zero all modes from N_s to N and thus the *correct* corresponding stationary distribution is, according to Eq. (B7),

$$\widehat{P}_{a_s}[\hat{h}] = \mathcal{N}_s^{-1} \exp\left(-\frac{1}{2} \frac{\nu}{DL a_s^2} \sum_{n=-N_s/2}^{N_s/2} |\hat{h}_{q_n} (1 - e^{iq_n a})|^2\right). \quad (\text{B8})$$

On the other hand, had we started from the ‘‘smoothed’’ lattice and constructed the differences $\delta h_i^s = h_i^s - h_{i+b}^s$ of the coarse-grained heights, we would have found

$$\widehat{P}_{a_s}[\hat{h}] = \mathcal{N}_s^{-1} \exp\left(-\frac{1}{2} \frac{\nu}{DL a_s^2} \sum_{n=-N_s/2}^{N_s/2} |\hat{h}_{q_n} (1 - e^{iq_n b a})|^2\right), \quad (\text{B9})$$

which differs from the previous expression.

It is clear that this is a general problem of all discretizations in real space. In the limit $a \rightarrow 0$, in fact, one recovers from Eq. (B9) the correct expression (B4).

-
- [1] A. S. Weigend and N. A. Gershenfeld, *Time Series Prediction* (Addison-Wesley, Reading, MA, 1994).
- [2] H. D. Abarbanel, R. Brown, J. J. Sidorowitch, and L. S. Tsimring, *Rev. Mod. Phys.* **6**, 1331 (1993).
- [3] E. J. Kostelich and T. Schreiber, *Phys. Rev. E* **48**, 1752 (1993).
- [4] See, e.g., C. W. Gardiner *Handbook of Stochastic Methods*, 2nd ed. (Springer-Verlag, Berlin, 1990); N. G. van Kampen *Stochastic Processes in Physics and Chemistry* (North-Holland, Amsterdam, 1992).
- [5] L. Battiston and M. Rossi, *Int. J. Bifurcation Chaos and Appl. Sci. Eng.* **5**, 310 (2000).
- [6] M. Kardar, G. Parisi, and Y. C. Zhang, *Phys. Rev. Lett.* **56**, 889 (1986).
- [7] For recent reviews, see e.g., J. Krug, *Adv. Phys.* **46**, 139 (1997); A. L. Barabasi and H. E. Stanley, *Fractal Concepts in Surface Growth* (Cambridge University Press, Cambridge, 1995); T. Halpin-Haley and Y. C. Zhang, *Phys. Rep.* **254**, 215 (1995); M. Marsili, A. Maritan, F. Toigo, and J. R. Banavar, *Rev. Mod. Phys.* **68**, 963 (1996); P. Meakin, *Phys. Rep.* **235**, 131 (1993).
- [8] S. F. Edward and D. R. Wilkinson, *Proc. R. Soc. London, Ser. A* **381**, 17 (1982).
- [9] D. A. Huse and C. Henley, *Phys. Rev. Lett.* **54**, 2708 (1985).
- [10] D. Forster, D. R. Nelson, and M. J. Stephen, *Phys. Rev. A* **16**, 732 (1977).
- [11] V. Yakhot, *Phys. Rev. A* **24**, 642 (1981).
- [12] B. Bogosian, C. C. Chow, and T. Hwa, *Phys. Rev. Lett.* **83**, 5262 (1999).
- [13] C. Lam and L. M. Sander, *Phys. Rev. Lett.* **71**, 561 (1993).
- [14] C. Lam and F. G. Shin, *Phys. Rev. E* **58**, 5592 (1998).
- [15] H. Risken, *The Fokker-Planck Equation* (Springer-Verlag, Berlin, 1989).
- [16] M. Beccaria and G. Curci, *Phys. Rev. E* **50**, 4560 (1994).
- [17] T. J. Newman and M. R. Swift, *Phys. Rev. Lett.* **79**, 2261 (1997).
- [18] T. J. Newman and A. J. Bray, *J. Phys. A* **29**, 7917 (1996).
- [19] C. Lam and F. G. Shin, *Phys. Rev. E* **57**, 6506 (1998).
- [20] R. Mannella, in *Noise in Nonlinear Dynamical Systems*, edited by F. Moss and P. V. E. McClintock (Cambridge University Press, Cambridge, England, 1989), Vol. 3.
- [21] A correct discretization was also previously obtained by A. Maritan (private communication).
- [22] See, e.g., N. Goldenfeld *Lectures on Phase Transitions and the Renormalization Group* (Addison-Wesley, Reading, MA, 1993), p. 226.